THE EFFECTS OF FINITE ELEMENT GRID DENSITY ON MODEL CORRELATION AND DAMAGE DETECTION OF A BRIDGE

BY

Todd Simmermacher
R.L. Mayes
G. M. Reese
G. H. James
Sandia National Laboratories
Albuquerque, NM 87185

D. C. Zimmerman
Dept. of Mechanical Engineering
University of Houston
Houston, TX 77204

An Extended Abstract Presented for Consideration for Inclusion in the

AIAA Adaptive Structures Conference

April 13-14, 1995

New Orleans, LA

DISCLAIMER

DISCLAIMER

Portions of this document may be illegible in electronic image products. Images are produced from the best available original document.

The Effects of Finite Element Grid Density on Model Correlation and Damage Detection of a Bridge

Todd Simmermacher
R. L. Mayes
G. M. Reese
G. H. James
Sandia National Laboratories
Albuquerque, NM 87185

David Zimmerman
Dept. of Mechanical Engineering
University of Houston
Houston, TX 77204

Abstract

Variation of model size as determined by grid density is studied for both model refinement and damage detection. In model refinement, it is found that a large model with a fine grid is preferable in order to achieve a reasonable correlation between the experimental response and the finite element model. A smaller model falls victim to the inaccuracies of the finite element method. As the grid become increasing finer, the FE method approaches an accurate representation. In damage detection the FE method is only a starting point. The model is refined with a matrix method which doesn't retain the FE approximation, therefore a smaller model that captures most of the dynamics of the structure can be used and is preferable.

Introduction

Large finite element models are typically used to represent modern structures. The size of the model can come from either representation of the many different parts of the structure or a fine level of discretization. As grid density increases, the model ideally converges to an accurate representation of the behavior of the actual structure or at least more accurately represents the dynamics of the structure. However, as the grid density increases, the model size also increases, demanding more computing power to evaluate the model. Also, although using a very fine mesh increases model accuracy, some form of model correlation will still have to be performed to correct for inaccurate parameters such as modulus or density, or uncertain parameters such as springs at an interface.

Model correlation and model based damage detection, while related, have very different objectives. Model correlation is performed to adjust an FE model response to approach the experimental response of the structure. The correlated model is then used as an analytical tool for stress/strain analysis, control law development, response to untested conditions, etc. For damage detection, the model must very accurately represent an experimental data set. This accurate representation of the structure will be used as a baseline to determine changes in the mechanical characteristics of the actual structure that result from fatigue, corrosion, unplanned impact, etc.

All the techniques found in the literature can be used for both damage detection and model refinement. In practice, however, model correlation is usually performed with an algorithm that adjusts the physical parameters such as density in order for the

correlated model to remain finite element consistent. In contrast, damage detection is typically performed with a matrix update method which does not maintain finite element consistency. Survey papers providing an overview of methods of both damage detection and model correlation are provided by Ibrahim [1], and Heylen [2].

A popular method of model correlation is the use of Design Sensitivities (DS) to drive the variation of a given set of parameters. Through a wise choice of parameters and a FE model that represents all relevant behavior of the system, the model can be adjusted to accurately represent the actual structure. The use of DS involves some sort of optimization. Least Squares methods [3] and, more recently Genetic algorithms [4], have been used successfully to correlate models.

Matrix methods for damage detection can be divided into three categories: optimal matrix updates, eigenstructure assignment methods, and minimum rank perturbation techniques. Optimal matrix update methods calculate the change in the property matrices (mass, stiffness, and/or damping) that minimize a given cost function, typically defined with a Frobenious norm, subjected to various constraints. These constraints can include satisfaction of the eigenvalue problem, conservation of a given sparsity, definiteness of property matrices, etc. [5] [6]

Eigenstructure assignment techniques find the pseudo control that will bring the model into agreement with the test data. The pseudo control is then used as a correction to the property matrices. By inspecting the changes in the property matrices, the extent of damage can be determined.[7] [8]

Minimum Rank Perturbation Theory (MRPT) has been developed as a computationally efficient method of determining the extent and location of damage in a structure. By constraining the rank of the perturbation matrix, an accurate assessment of the extent of damage can be made. The rank constraint has been found to be consistent with many forms of damage that occur in practice. [9] [10]

A tradeoff exists between the level of discretization used in a FE model and the size of the resulting model. The question that arises is "When is the grid fine enough?". Since model correlation and damage detection have different objectives, it is reasonable to believe that different mesh resolution would be necessary for each problem. In this paper, the question of discretization is addressed in both the model correlation and the damage detection problem. The structure used is a portion of the I-40 bridge over the Rio Grande which was extensively tested by Farrar et al [11]. The models range from a simple 26 node beam and plate model, to a 2682 DOF (Degree of Freedom) model. The same models are used for both the model correlation and the damage detection, for comparison.

Model Correlation Theory

The model correlation was performed using PEGA [4],[12] which utilizes the sensitivity approach coupled to a genetic algorithm optimizer. The genetic algorithm is used because of the possibility of local minima in the solution space. The sensitivity

approach uses the design sensitivities of the eigenvalues with respect to the chosen parameters to determine corrections to the parameters based upon the linear approximation

$$\varphi_{new} = \varphi_o + \frac{\partial \varphi}{\partial p} \Delta p \qquad (1)$$

where φ_{new} are the experimental frequencies, φ_o are the frequencies of the FE model and p is a vector of parameters chosen to vary. The rectangular matrix $(\partial\varphi/\partial p)$ is known as the design sensitivity matrix and can be determined by MSC/NASTRAN [13].

PEGA uses Equ. (1) to approximate the new φ_o for the evaluation of the Fitness Index which is defined as

$$FI = \left\{ \sum_{i=1}^{m} \left(w_i^f \left| \frac{\varphi_o^i - \varphi_{new}^i}{\varphi_{new}^i} \right| \right) \right\} \qquad (2)$$

where w^f are used to weight the individual frequencies.

Figure 1 shows a flow chart that describes the correlation procedure. The models are correlated by a combination of running PEGA which produces changes in the chosen parameters and running MSC/NASTRAN to update the model. A one to one correspondence between the analytical and experimental frequencies is obtained by calculating the Modal Assurance Criterion (MAC) using the analytical and experimental mode shapes. Although PEGA produces an estimate of the updated natural frequencies of the model, these estimates are typically in error and a full run of MSC/NASTRAN is necessary for an evaluation of the correlation. This cycle is repeated until the model has converged. As indicated in [4], when the model form has been properly defined, convergence requires less than ten iterations.

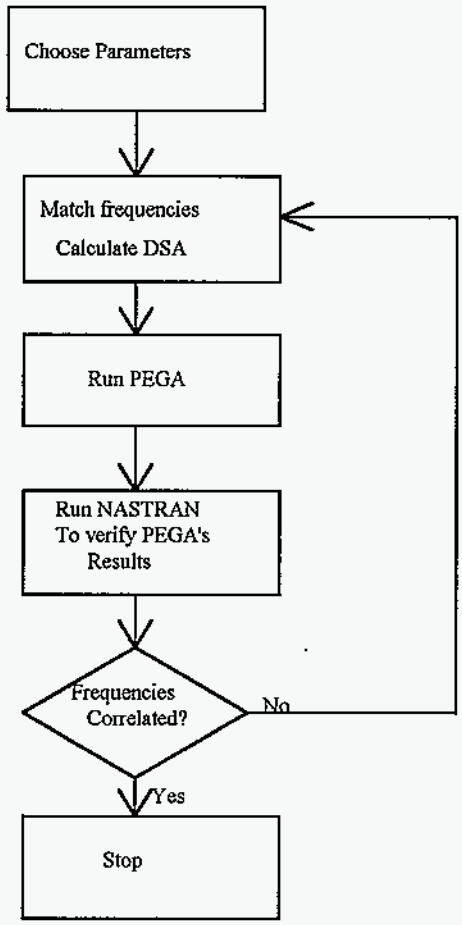

Figure 1. Flow chart for PEGA iterations.

Damage Detection Theory

The goal for the I-40 bridge was to determine if damage was present and, if so, locate the damage, not estimate the extent. The objective was to reduce the work load of an inspection team. If the damage can be determined to lie within a certain area, the inspection team can concentrate its efforts to that area. For this work, MRPT was used for the damage detection which uses modal characteristics of the assumed damage structure and compares them with a baseline model which has been correlated with the bridge in some assumed healthy state. MRPT was used originally to correlate the model for the damage detection portion of this work. The model was linear although the damage was typically non-linear.

The model correlation portion of damage detection is different from the typical definition of model correlation. Here the updated model must match the "healthy" experimental data exactly so that errors in the model are not wrongly interpreted as changes in the structure's health. A parameter based update, while powerful, will rarely allow the FE model's response to exactly match the test data. Matrix methods, specifically

MRPT, can exactly place the measured modes in the model assuming the form of the model is a least approximately correct.

The damage detection correlation involves correlating both the mass and stiffness matrix to the experimental data. A brief discussion of the procedure will be provided here with the details being found in Zimmerman and Kaouk [9].

The measure test data is assumed to satisfy

$$(M_a - \Delta M)V_{test}\omega^2_{test} + (K_a - \Delta K)V_{test} = 0 \tag{3}$$

where M_a and K_a are the original mass and stiffness matrices, ΔM and ΔK are the perturbation matrices sought that correct the analytic model to match the experimental response, V_{test} is the matrix of mass normalized measured mode shapes and ω^2_{test} is a diagonal matrix of the measured frequencies squared. If the known information is grouped on one side of the equal sign and the unknowns on the other, two matrices B_m and B_k can be defined

$$M_a V_{test}\omega^2_{test} + K_a V_{test} = \Delta M V_{test}\omega^2_{test} + \Delta K V_{test} = B \tag{4}$$

If B can be decomposed into B_m and B_k as follows

$$\begin{aligned} B &= B_m\omega^2_{test} + B_k \\ \Delta M V_{test} &= B_m \\ \Delta K V_{test} &= B_k \end{aligned} \tag{5}$$

ΔM and ΔK can be calculated using MRPT as

$$\begin{aligned} \Delta M &= B_m\left(B_m^T V_{test}\right)^{-1} B_m^T \\ \Delta K &= B_k\left(B_k^T V_{test}\right)^{-1} B_k^T \end{aligned} \tag{6}$$

The inversion is possible if B_m and B_k are of full rank.

The ΔM and ΔK as calculated in Equ. (6) have a few properties that make them attractive for damage detection. One property is that the correction to M_a and K_a, Equ. (6), will exactly place the experimental modes into the analytical model because they will satisfy Equ (3). Another property is that the corrected mass and stiffness matrices (M_a-Δ M) and (K_a-ΔK) will be symmetric. This was shown in [9].

A very significant property is that the zero/non zero pattern of B is reflected in ΔM and ΔK. Determining the location of damage requires the inspection of the zero/non zero pattern of the dynamic residual, B. If a degree of freedom is affected by damage, a non zero value will be present at that DOF in B. If that DOF is not affected by damage, a zero

will be at that location. Typically noise and model errors will be present making each entry in B be non zero, therefore "large" values are taken as damaged DOFs.

A final property is that the rank of ΔM and ΔK will be equal to the number of modes used for the calculation of B. This rank constraint allows the adjustment of the rank of ΔM and ΔK by a choice of the number of modes to use. The rank constraint has been found to be consistent with many forms of damage that are typically encountered.

Clearly there is an infinite set of B_m 's and B_k 's that satisfy

$$B = B_m \omega_{test}^2 + B_k \tag{7}$$

To arrive at a unique solution, physically meaningful constraints must be enforced. Two constraints come from the orthogonality conditions. The mass normal measured modal data must satisfy

$$\begin{aligned} V_{test}^T (M_a - \Delta M) V_{test} &= I \\ V_{test}^T (K_a - \Delta K) V_{test} &= \omega_{test}^2 \end{aligned} \tag{8}$$

By rearranging the orthogonality equations as before, separating the known quantities and the unknown quantities and comparing the result with Equ. 5, Equ. 8 becomes

$$\begin{aligned} V_{test}^T \Delta M V_{test} &= V_{test}^T M_a V_{test} - I = V_{test} B_m \\ V_{test}^T \Delta K V_{test} &= V_{test}^T K_a V_{test} - \omega_{test}^2 = V_{test} B_k \end{aligned} \tag{9}$$

The pseudo inverse could be used at this point to solve for B_m and B_k, however, that would destroy the important zero/non zero pattern of the resulting B_m and B_k. To preserve the zero/non zero pattern a formulation similar to the one used to derive Equ. (6) is used. A matrix P is to be found which satisfies

$$P(V_{test}^T B) = B \tag{10}$$

which can be found by

$$P = B(V_{test}^T B)^{-1} \tag{11}$$

so the decomposition of B can be performed as

$$\begin{aligned} B_m &= P(V_{test}^T M_a V_{test} - I) \\ B_k &= P(V_{test}^T K_a V_{test} - \omega_{test}^2) \end{aligned} \tag{12}$$

The calculation of ΔM requires that the modes be mass normal. Measured modes can be mass normalized if the driving point of the structure in question is measured.

Otherwise, if it is felt that the mass matrix represents the mass of the structure fairly well, the modes can be made mass normal by

$$V^i_{test_{normal}} = V^i_{test}((V^i_{test})^T M_a V^i_{test})^{-\frac{1}{2}} \tag{13}$$

Note that Equ. (13) does not affect the orthogonality of the modes, only the scaling. Although the measured modes of the bridge were experimentally extracted to be mass normal, Equ. (13) was used to force the modes to be mass normal to the analytical model. This was necessary due to confusion in the units of the measured data.

The damage inflicted on the I-40 bridge consisted of making increasingly larger cuts in one of the two plate girders supporting the road bed (Fig. 2). The first cut was a 2 ft vertical cut in the center of the web. The second cut extended down to the top of the lower flange. The third cut was made through half of the lower flange. The final cut severed the lower flange. The cuts did not remove any significant mass and therefore can be modeled as only a decrease in stiffness.

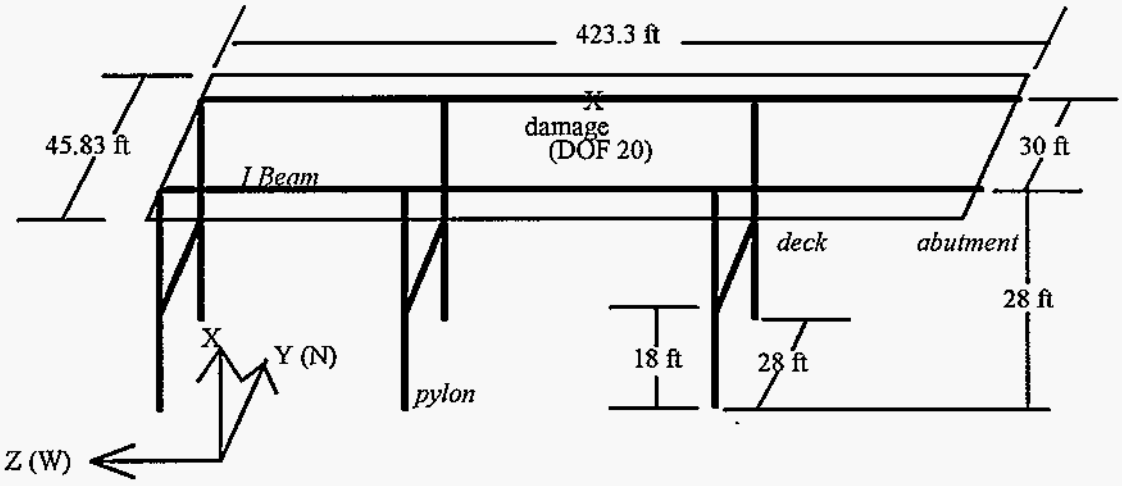

Figure 2. Bridge Model Schematic

Two definitions of the dynamic residual are used in this work. The first definition of the dynamic residual uses the assumption that the damage only affects the stiffness matrix and is defined as

$$M_h V_d \omega_d^2 + K_h V_d = \Delta K V_d = B \tag{14}$$

where the subscript h refers to the model correlated to the healthy data as described in Equ. (6) and the subscript d refers to the modal data of the damaged structure. The second definition assumes that both the mass and the stiffness matrices change and uses Equ (12) to define B_m and B_k, with B_k being used for locating damage. The thought here is that by separating mass and stiffness effects the noise in B_k will be reduced.

Noise in the measurements tends to mask damage in any one of the columns of any of the B matrices defined above. In order to compress the information in all of the modes a singular value decomposition can be performed on B and the location of damage can be determined by inspecting the zero/non zero pattern of the first p left singular vectors, where p is the rank of B determined from an inspection of the singular values.[10]

Areas that are stiff relative to the rest of the structure also cause problems in locating damage. Noise in the measurements is magnified by the large value associated with stiff elements which can swamp out the actual damage location. For example, a structure with a global stiffness on the order of 10^6 may have a localized stiffness on the order of 10^9. Assume a noise level of 2% and a damage level in the less stiff region of 20%. The 2% noise in the stiff region gives a stiffness variation on the order of $2x10^7$ while the damage in the less stiff region only has a variation of $2x10^5$. The damage would not be apparent unless some form of scaling is present. In this work the scaling used is defined as

$$\hat{B} = WB \tag{14}$$

where

$$W = \mathrm{diag}\left(\frac{1}{\|z^1\|}, \frac{1}{\|z^2\|}, \frac{1}{\|z^3\|}, \ldots, \frac{1}{\|z^n\|}\right) \tag{15}$$

and

$$Z = \begin{bmatrix} z^1 \\ z^2 \\ z^3 \\ \vdots \\ z^n \end{bmatrix} = (M_h \omega_d^2 + K_h) \tag{16}$$

In the bridge model, the pylons are areas of large stiffness when compared to the stiffness of the two plate girders. Without this weighting, damage is always located at the pylons.

Description of Models

Two different models were used for this study. The only difference between the models used for correlation and the models used for damage detection is that the damage detection models have the Y translations and the X rotations grounded to prevent out of plane motion, whereas the model correlation models have the full 6 DOF/node (Fig 2). The measurements were only in the X direction and the modes of interest have very small components in the Y translation and the X rotation. Sensors used for the collection of the experimental data consisted of 13 X direction accelerometers equally spaced along each of

the main plate girders for a total of 26 measurements. Only the first six modes were measured. The number of DOFs for each model given below refer to the model correlation model.

The large model (2682 DOFs) consisted of the roadbed as modeled with CQUAD4 elements, each of the two main plate girders divided into 48 CBAR elements, and each of the three pylon assemblies are divided up into 3 CBAR elements. Springs connect the pylons to the two plate girders and connect the roadbed to the ground in the X and Y directions at the abutment .

The small model (108 DOFs) consisted of one CBAR element between each of the sensor locations for the two plate girders, a roadbed made up of 12 CQUAD4 elements, crossbars between the two main plate girders at the sensor locations, and springs to ground to represent the pylons and the connection of the roadbed to the ground at the abutment.

Model Correlation Results

The first six modes were correlated with PEGA. The parameters chosen to vary in the optimization are the modulus of elasticity and thickness of the road bed, all the spring constants, the two principal moments of inertia of the two main plate girders, the two principal moments of inertia and the cross sectional area of each of the pylons, the two principal moments of inertia and the cross sectional area for the beams connecting the pylons, and an added mass term to account for crash barriers that were present on the road bed for a total of 27 design variables. All correlations are done using the data from the first damage case.

The results for the large model are shown in Table 1. Four iterations were required to get convergence of the frequencies. Most of the frequencies show good correlation. The exception is modes four and five which are close in frequency. During the correlation process they often required reordering. These two modes are closely spaced and tend to want to switch. In some of the experimental data, it was not possible to differentiate between these two modes.

Table 1. Change in large model's frequencies (Hz)

Mode	Initial Frequency	Final Frequency	Experimental
1	2.21	2.45	2.51
2	2.71	3.05	2.98
3	3.29	3.66	3.56
4	3.47	4.17	4.12
5	3.60	4.11	4.20
6	4.17	4.67	4.66

The results for the small model are shown in Table 2. Four iterations were also performed on the small model. The second and third modes in the small model were switched from the first iteration and never corrected. The small model had the most trouble predicting the higher frequencies. All six mode shapes were predicted in the model. Since the mesh is so coarse, only the general motion of the bridge could be predicted.

Table 2. Change in small model's frequencies (Hz)

Mode	Initial Frequency	Final Frequency	Experimental
1	2.08	2.21	2.51
2	3.42	3.46	2.98
3	3.18	3.37	3.56
4	3.90	4.12	4.12
5	5.00	4.74	4.20
6	6.01	5.87	4.66

Damage Detection Results

The detection of the location of damage was performed using the MRPT results presented above. Each model was reduced to the sensor set DOF (X translation), producing a model with 26 degrees of freedom. The reduction method used was the Guyan reduction [14]. Once the original model was reduced, the mass and stiffness

matrices were updated using the first damage case data as was shown in the Model Correlation section. In general, the large model did not perform as well as the smallest model in locating the damage. This is due to the inaccuracies in the reduction procedure. Guyan reduction does not accurately reduce the mass matrix if a large amount of inertia is present at the omitted DOFs. A poor representation of the mass matrix results, diminishing the ability to locate damage. Currently, other techniques of reduction are being explored as well as eigenvector expansion methods.

There were many problems identifying the modes from the experimental data. There were 12 other bridge sections of similar construction all within close proximity of the test section. Each other section was excited by traffic and, therefore, corrupted the measurements producing clusters of modes around each peak. The test consisted of testing one of the three spans over the Rio Grande. The other two spans were in the process of being demolished while the tests were being performed. This can be viewed as an unquantifiable change in the boundary conditions, further corrupting the measurements.

The large model required the removal of 1762 degrees of freedom from the model. The mass matrix for this system can be expected to be a poor representation of the original mass of the system due once again to the Guyan reduction. The damage was located near DOF 20. Figures 3 and 4 show the scaled left singular vectors for the two most severe cases of damage. Moving left to right in Fig 3, the most severe case of damage, the first and third scaled B vectors show the damage clearly at the proper location whereas the second and remaining vectors do not clearly indicate a damaged location. Similarly for B_k, only the second and third vector indicate damage at the correct location. The first left singular vector contains the most information about the condition of the bridge. The first left singular vector in both B and B_k indicate that the first DOF may be affected by damage. Both B and B_k for the third damage case (Fig. 4) show no clear or consistent indication of damage.

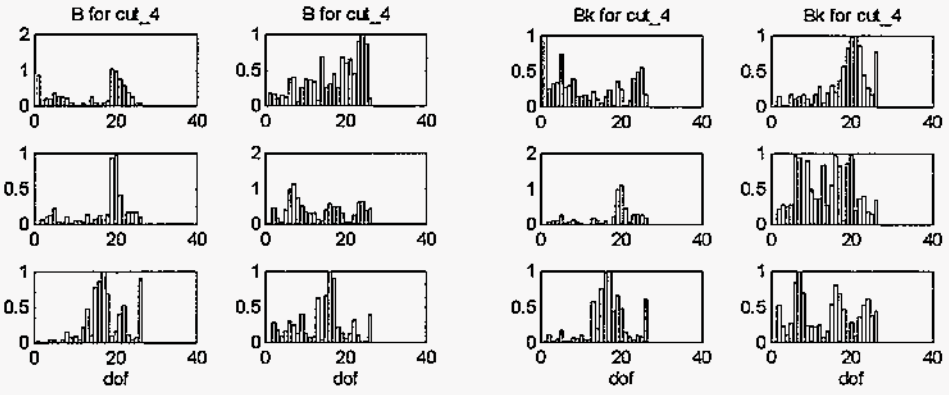

Figure 3. Scaled B and B_k vectors for fourth damage case (large model)

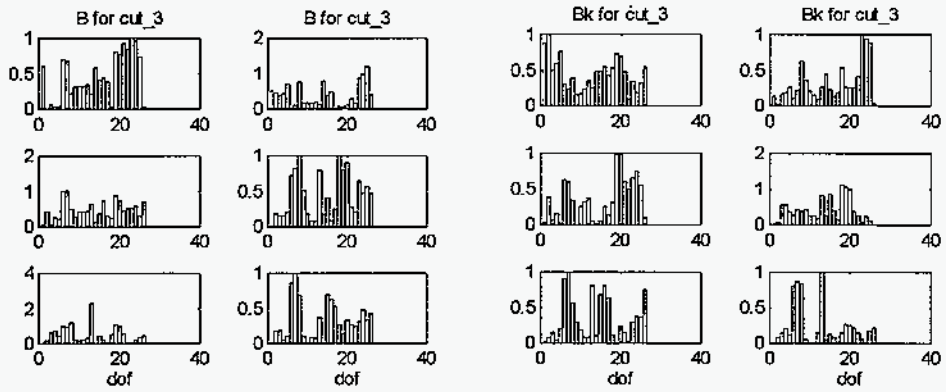

Figure 4. Scaled B and B_k vectors for third damage case (large model)

The small damage model only required the removal of 52 degrees of freedom. It would be expected that the reduced mass matrix would more accurately represent the actual mass of the system. Figures 5 and 6 display the modified B and B_k vectors for the small model. The correct damage is clearly indicated in the first four scaled left singular vectors of the B for the fourth damage case (Fig. 5). For B_k, only the first two and the fourth scaled left singular vectors clearly show the proper damage. For the third damage case (Fig. 6), the B vector shows no consistent or clear indication of damage. The first scaled left singular B_k vector shows damage at DOF 20, the actual location.

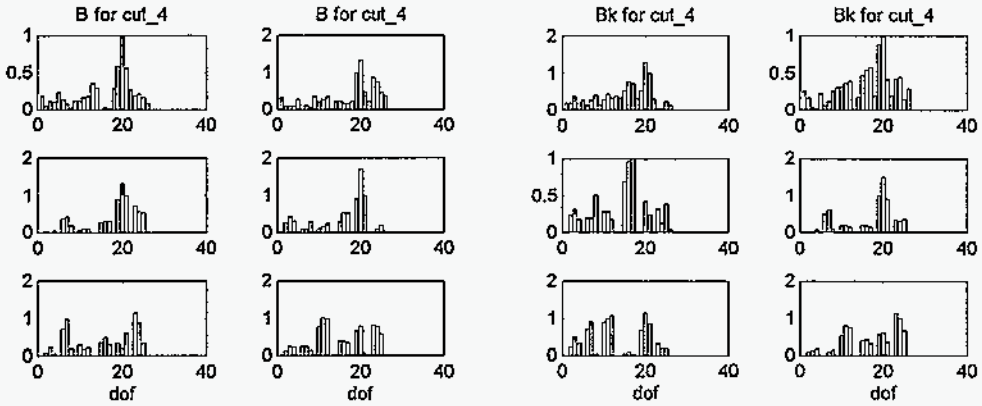

Figure 5. Scaled B and B_k vectors for fourth damage case (small model)

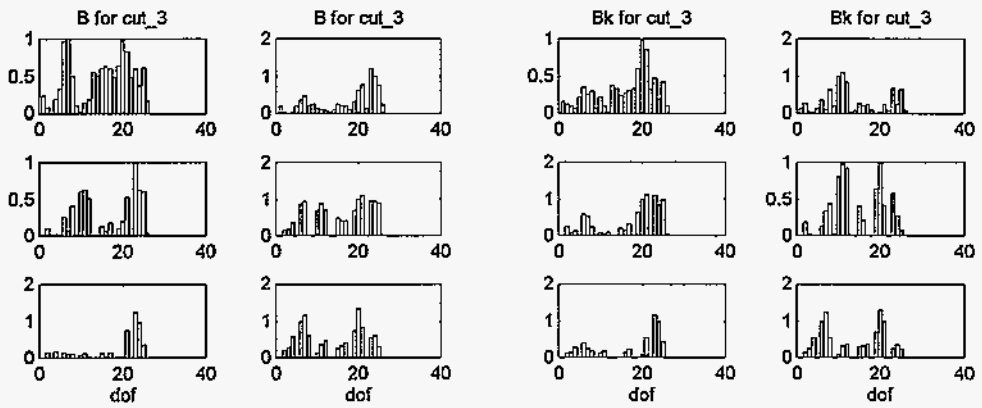

Figure 6. Scaled B and B_K vectors for third damage case (small model)

Discussion

The model correlation process as used here varies design parameters such as density to adjust a finite element model to approximate an experimental response. The model remains a finite element approximation. Typically with finite element models, a finer mesh will result in a better correlation. With a finer mesh, the FE approximation is more exact and with a finer mesh there can be more design parameters to include in a correlation. This gives the model more degrees of freedom to be adjusted.

The larger model of the I-40 bridge, after correlation, did represent the experimental frequencies better than the small model, especially at higher frequencies. The mode shapes, however, were accurately represented in both models. For a basic understanding of the characteristics of the bridge a coarse mesh model is sufficient while for any detailed work, the more refined mesh would be more appropriate.

For damage detection, it is the fact that the small model can accurately represent the mode shapes that allows it to be useful. The model is first reduced then corrected using MRPT that places the measured modes in the model exactly. Since the mode shapes are predicted, the corrections to the model are mainly to fix the frequencies. The larger models, however, are greatly corrupted by the Guyan reduction process and the large changes that MRPT produces in the mass and stiffness matrices adversely affects any structure that was present in the model to begin with.

Conclusions

Large and small models are compared from the viewpoint of model correlation and damage detection. For model correlation, large models are necessary to reduce the effects of the discretization error inherent in the finite element method. For damage detection, a small model that captures the approximate nature of the structure, such as mode shapes, is sufficient and can be preferable. Use of a large model for damage detection will require either a large amount of DOFs to be removed via some reduction method or require a large portion of the mode shapes to be approximated with some expansion process.

Acknowledgments

This work was supported by the United States Department of Energy under contract DE-AC04-94AL85000.

References

[1] Ibrahim, S. R. and Saafan, A. A., "Correlation of Analysis and Test in Modeling of Structures, Assessment and Review", Proceedings of the 5th International Modal Analysis Conference, pp 1651-1660, 1987.

[2] Heylen, W. and Sas, P. "Review of Model Optimization Techniques", Proceedings of the 5th International Modal Analysis Conference, pp 1177-1182, 1987.

[3] Martinez, D., Red-Horse, J., and Allen, J."System Identification Methods for Dynamic Structural Models of Electronic Packages", Proceedings of the 32nd SDM Conference, Baltimore, MD, pp 2336-2346, 1991.

[4] Fulcher, C. W., Marek, E. L., and Mayes, R. L., "Test/Analysis Correlation and Model Updating of the STARS I & II Missile Systems", NAFEMS International Conference on Structural Dynamics Modeling Test, Analysis, and Correlation, Milton Keynes Conference Centre, UK, July 1993.

[5] Baruch, M., and Bar Itzhack, I. Y., "Optimum Weighted Orthogonalization of Measured Modes", AIAA Journal, Vol. 16, No. 4, pp 346-351, 1978.

[6] Smith, S. W., and Beattie, C. A., "Secant-Method Adjustment Using Modal Data", AIAA Journal, Vol. 29, No. 1, pp. 119-126, 1991.

[7] Zimmerman, D. C., and Widengren, W.,"Model Correction Using a Symmetric Eigenstructure Assignment Technique", AIAA Journal, Vol. 28, No. 9, pp 1670-1676, 1990.

[8] Zimmerman, D. C., and Kaouk, M, "Eigenstructure Assignment Approach for Structural Damage Detection", AIAA Journal, Vol. 30, No. 7, pp 1848-1855, 1992.

[9] Zimmerman, D. C., and Kaouk, M, "Structural Damage Detection Using a Minimum Rank Update Theory", Accepted for Publication ASME Journal of Vibration and Acoustics.

[10] Zimmerman, D. C., and Simmermacher, T. W. "Model Refinement and System Health Monitoring Using Data from Multiple Static Loads and Vibration Tests", Proceedings of the Dynamic Specialists Conference, Hilton Head, SC, 1994.

[11] Farrar, C.R., Baker, W.E., Bell, T.M., Cone, K.M., Darling,T.W., Duffey, T.A., Eklund, A., Migliori, A., "Dynamic Characterization and Damage Detection in the I-40

Bridge Over the Rio Grande", Los Alamos National Laboratories Report No. LA-12767-MS, 1994.

[12] Reese, G. M. "PEGA: Parameter Estimation Using the Genetic Algorithm", Users' Guide, Internal Report, Sandia National Laboratories, 1993.

[13] MacNeal-Schwendler Corp.,"MSC/NASTRAN Users' Manual", V. 66, 1988.

[14] Guyan, R. J., "Reduction of Stiffness and Mass Matrices" AIAA Journal, Vol, 3, No. 2, pg. 380, 1965.